

DETECTABILITY OF PAIR ECHOS FROM GAMMA-RAY BURSTS AND INTERGALACTIC MAGNETIC FIELDS

KEITARO TAKAHASHI^{1,*}, KOHTA MURASE¹, KIYOTOMO ICHIKI², SUSUMU INOUE³, SHIGEHIRO NAGATAKI¹

Draft version October 22, 2018

ABSTRACT

High-energy emission from gamma-ray bursts (GRBs) can give rise to pair echos, i.e. delayed inverse Compton emission from secondary e^\pm pairs produced in $\gamma-\gamma$ interactions with intergalactic background radiation. We investigate the detectability of such emission with modern-day gamma-ray telescopes. The spectra and light curves are calculated for a wide range of parameters, applying the formalism recently developed by Ichiki et al. The flux depends strongly on the unknown magnitude and coherence length of intergalactic magnetic fields, and we delineate the range of field strength and redshift that allow detectable echos. Relevant uncertainties such as the high-energy cutoff of the primary gamma-ray spectrum and the intensity of the cosmic infrared background are addressed. GLAST and MAGIC may be able to detect pair echo emission from GRBs with redshift $\lesssim 1$ if the primary spectra extend to ~ 10 TeV.

Subject headings: magnetic fields — gamma rays: bursts — radiation mechanisms: nonthermal

1. INTRODUCTION

Gamma-ray bursts (GRBs) are expected to be emitters of high-energy gamma-rays, possibly up to TeV energies and above. Such TeV photons can interact with photons of the cosmic infrared background to produce electron-positron pairs, which in turn generate secondary inverse Compton gamma-rays in the (1 – 100) GeV range that arrive with a characteristic time delay. Hereafter we shall call such delayed secondary emission "pair echos". Pair echo emission has attracted much attention as a powerful tool to probe high-energy emission of GRBs because its detection would directly prove that the spectrum of the GRB emission extends to TeV range.

So far, the observations of high-energy gamma-rays from GRBs have been limited. There are some detections of GeV gamma-rays by EGRET (Sommer et al. 1994; Hurley et al. 1994), while only upper bounds have been obtained for TeV range (Albert et al. 2006; Abdo et al. 2007), although some tentative detections have been claimed (The Tibet As Gamma Collaboration et al. 1996; Padilla et al. 1998; Atkins et al. 2000). Thus, it is not clearly known observationally whether the spectrum extends to TeV region. On the other hand, high energy emission of GRBs has been studied theoretically by many authors and the spectrum depends highly on the emission mechanism and physical parameters. In the conventional internal shock model where prompt emission is attributed to synchrotron radiation from electrons, TeV gamma rays can be produced via leptonic mechanisms (Papathanassiou & Meszaros 1996; Guetta & Granot 2003; Asano & Inoue 2007) and/or hadron-related mechanisms (Totani 1998; Pe'er & Waxman 2004; Dermer & Atoyan 2004; Asano & Inoue 2007; Murase et al. 2008). Although these high-energy gamma rays can suffer from the pair-creation process within the source, they can escape from the source if the emission radius and/or bulk Lorentz factor are large enough (Razzaque et al. 2004;

Murase & Ioka 2008). Hence, as long as the conventional internal shock model is valid, we may expect that at least some fraction of GRBs have spectra extended to TeV region.

Plaga (1995) proposed that pair echo emission can also probe intergalactic magnetic fields because the delay time and the flux depends strongly on their magnitude and coherence length. Duration and spectra of pair echos from GRBs including the effects of magnetic fields have been studied in subsequent works (Dai & Lu 2002; Wang et al. 2004; Razzaque et al. 2004; Ando 2004; Casanova et al. 2007; Murase et al. 2007) and revealed that intergalactic magnetic fields as tiny as $\sim 10^{-20}$ G could be probed by its observation. In our previous work (Ichiki et al. 2007), we constructed an analytic model which properly incorporates geometrical effects of particle paths on time delay. It allow us to calculate the time evolution of pair echos more precisely than other simple analyses presented by Dai et al. (2002).

Plaga's method is currently the only way to probe such tiny magnetic fields, while other methods utilizing Faraday rotation or cosmic microwave background are sensitive to magnetic fields of order 1 nG. Actually, presence of tiny intergalactic magnetic fields have been predicted by several mechanism, such as inflation (Turner & Widrow 1988; Bamba & Sasaki 2007), reionization (Gnedin et al. 2000; Langer et al. 2005) and density fluctuations (Matarrese et al. 2005; Takahashi et al. 2005; Ichiki et al. 2006; Takahashi et al. 2007; Maeda et al. 2008), and observation of intergalactic magnetic fields would give important information on the origin of galactic magnetic fields (Widrow 2002).

It would be important to argue the detectability of pair echo emission from GRBs for ongoing ground-based instruments such as MAGIC, which we take as a representative of this type, H.E.S.S., VERITAS, CANGAROO III and MILAGRO, and an upcoming satellite GLAST. There are several factors concerning the detectability: (1) the object must emit TeV-gamma-rays which lead to pair echo emission, (2) the flux of pair echos must be higher than detector sensitivity, (3) the pair echo emission must not be masked by other emission such as afterglow. Concerning the point (1), we just assume the cut-off energy, E_{cut} , of the primary spectrum. Our main subject is the point (2). The flux of pair echo emission depends on,

¹ Yukawa Institute for Theoretical Physics, Kyoto University, Oiwake-cho, Kitashirakawa, Sakyo-ku, Kyoto, 606-8502, Japan

² Research Center for the Early Universe, University of Tokyo, 7-3-1 Hongo, Bunkyo-ku, Tokyo, 113-0033, Japan

³ Department of Physics, Kyoto University, Oiwake-cho, Kitashirakawa, Sakyo-ku, Kyoto, 606-8502, Japan

*keitaro@yukawa.kyoto-u.ac.jp

other than the distance to the GRBs and properties of magnetic fields, the amount of absorption of primary gamma-rays. It is determined by the spectrum of primary emission and the amount of CIB. We estimate, using our formalism to calculate spectra and light curves of pair echos, the detectability in (redshift)-(magnitude of magnetic fields) plane varying E_{cut} and CIB model.

Concerning the point (3), it should be noted that afterglows can also have high energy emission above GeV (Zhang & Mészáros 2001; Wang et al. 2001; Fan et al. 2008), although it has not been confirmed by observation either. Typically afterglow continues for several days so that its high energy emission can mask the pair echos. There have been many theoretical predictions on high-energy afterglow, but we postpone the comparison of spectra and lightcurves between afterglow and pair echos and give some comments in the last section.

In section 2, we summarize the basic elements of pair echo emission and the calculation formalism constructed in Ichiki et al. (2007), and apply the formalism to GRB cases to show the spectra and light curves for a wide range of parameters. Then, we argue the detectability of pair echo emission considering uncertainties in high-energy cutoff in primary spectrum and the density of cosmic infrared background in section 3. Finally we give a summary in section 4.

2. PAIR ECHO EMISSION

Let us summarize the basic elements of pair echo emission from high-energy gamma-ray sources. A gamma-ray with energy $E_\gamma \gtrsim 1$ TeV emitted from a source, called a primary gamma-ray, pair-annihilates with an ambient infrared photon to create an electron-positron pair with the mean free path, $\lambda_{\gamma\gamma} = 1/(0.26\sigma_T n_{\text{IR}}) = 19 \text{ Mpc}(n_{\text{IR}}/0.1 \text{ cm}^{-3})^{-1}$, where σ_T is the Thomson cross section and n_{IR} is the number density of infrared background. Created charged particles (electron or positron) have energies $E_e = E_\gamma/2$ and upscatter ambient CMB photons to produce high-energy secondary gamma-rays. The average energy of upscattered photons is, $\langle E_{\text{delay}} \rangle = 2.7 T_{\text{CMB}} \gamma_e^2 = 2.5 \text{ GeV}(E_\gamma/2 \text{ TeV})^2$, where $\gamma_e = E_e/m_e$ is the Lorentz factor of a charged particle and $T_{\text{CMB}} = 3 \text{ K}$ is the CMB temperature. We can see that, considering the energy range of the primary gamma-rays as $1 \sim 10 \text{ TeV}$, the typical energy range of pair echo emission is $1 \sim 100 \text{ GeV}$. The mean free path of charged particles is evaluated as, $\lambda_{\text{IC,scat}} = 1/(\sigma_T n_{\text{CMB}}) = 1.2 \text{ kpc}$, where $n_{\text{CMB}} \approx 420 \text{ cm}^{-3}$ is the number density of CMB. The charged particles scatter CMB photons successively until they lose most of their energy after propagating the cooling length, $\lambda_{\text{IC,cool}} = 3m_e^2/(4E_e\sigma_T U_{\text{CMB}}) = 350 \text{ kpc}(E_e/1 \text{ TeV})^{-1}$, where U_{CMB} is the CMB energy density. Note that ambient infrared photons should also be the target of IC scattering. They can be important for pair echo gamma-rays with $E_{\text{delay}} \gtrsim 10 \text{ GeV}$ and/or even lower energies at late time (Murase et al. 2007).

Pair echo emission is induced by angular spreading and magnetic fields. The direction of upscattered photons deviates from the original directions of the charged particle and primary gamma-ray by an angle $\sim 1/\gamma_e$ so that the typical delay time can be evaluated as,

$$\Delta t_{\text{ang}} \sim \frac{1}{2\gamma_e^2}(\lambda_{\gamma\gamma} + \lambda_{\text{IC,cool}}) \\ \sim 3 \times 10^2 \text{ sec} \left(\frac{E_{\text{delay}}}{1 \text{ GeV}} \right)^{-1} \left(\frac{n_{\text{CIB}}}{0.1 \text{ cm}^{-3}} \right)^{-1}. \quad (1)$$

If magnetic fields are present in the region of the propagation of charged particles, their directions are further deflected by magnetic fields. For weak magnetic fields with coherence length $r_{\text{coh}} (< \lambda_{\text{IC,cool}})$, the variance of the deflection angle due to magnetic fields is, $\sqrt{\langle \theta_{\text{B,random}}^2 \rangle} = \sqrt{\lambda_{\text{IC,cool}}/6r_{\text{coh}}}r_{\text{coh}}/r_L = 2.2 \times 10^{-6}(E_e/1 \text{ TeV})^{-3/2}(B/10^{-18} \text{ G})(r_{\text{coh}}/100 \text{ pc})^{1/2}$, where r_L is the Larmor radius, $r_L = 1.1 \text{ Gpc}(E_e/1 \text{ TeV})(B/10^{-18} \text{ G})^{-1}$. Then typical delay time due to magnetic deflection is,

$$\Delta t_{\text{B}} = \frac{1}{2}(\lambda_{\gamma\gamma} + \lambda_{\text{IC,cool}})\langle \theta_{\text{B,random}}^2 \rangle \\ \approx 2 \times 10^4 \text{ sec} \left(\frac{E_{\text{echo}}}{1 \text{ GeV}} \right)^{-3/2} \left(\frac{B}{10^{-18} \text{ G}} \right)^2 \\ \times \left(\frac{r_{\text{coh}}}{100 \text{ pc}} \right) \left(\frac{n_{\text{CIB}}}{0.1 \text{ cm}^{-3}} \right)^{-1}. \quad (2)$$

Eventually, the true delay time is $\Delta t = \max[\Delta t_{\text{ang}}, \Delta t_{\text{B}}]$ and we can probe magnetic field by measuring the time delay between primary and secondary emissions. Because the mean free path of the primary gamma-rays can be larger than the typical sizes of galaxy and cluster of galaxies, the primary gamma-rays will escape from the host galaxy /cluster of galaxies of the GRB before they pair-annihilate with ambient infrared photons. Therefore, the propagation region of charged particles will mostly be in void region and this is where we can expect to probe magnetic fields by our method.

In our previous study (Ichiki et al. 2007), the spectrum and light curves of pair echo from a GRB was investigated and let us summarize the basic formalism here. For a primary gamma-ray fluence dN_γ/dE_γ , the time-integrated flux of charged particles over the GRB duration can be written as,

$$\frac{dN_{e,0}}{d\gamma_e}(\gamma_e) = 4m_e \frac{dN_\gamma}{dE_\gamma}(E_\gamma = 2m_e\gamma_e) [1 - e^{-\tau_{\gamma\gamma}(E_\gamma = 2\gamma_e m_e)}]. \quad (3)$$

Note that we shall assume the GRB duration $T' = 50 \text{ s}$ in this letter. Here $\tau_{\gamma\gamma}(E_\gamma)$ is the optical depth to pair production for gamma-rays with energy E_γ . From this, the spectrum of the pair echo emission can be calculated as

$$\frac{d^2 N_{\text{echo}}}{dt dE_\gamma} = \int d\gamma_e \frac{dN_e}{d\gamma_e} \frac{d^2 N_{\text{IC}}}{dt dE_\gamma}. \quad (4)$$

where $d^2 N_{\text{IC}}/dt dE_\gamma$ is the IC power from a single electron. Here $dN_e/d\gamma_e$ is the total time-integrated flux of charged particles responsible for the pair echo emission observed at time t_{obs} after the burst and is nontrivially related to $dN_{e,0}/d\gamma_e$ in Eq. (3). The relation was calculated in Ichiki et al. (2007) taking geometrical effects due to random walks properly into account, which makes it possible to follow the time evolution of pair echo emission. Calculation needs numerical integration but it can be written roughly as, $dN_e/d\gamma_e = (\lambda_{\text{IC,cool}}/c\Delta t)dN_{e,0}/d\gamma_e$, as given by Dai et al. (2002).

Typical spectra and light curves of pair echo emission from GRBs are shown in Figs. 1 and 2. Here we assumed that the primary gamma-ray flux is power-law with index 2.2, that is, $dN_\gamma/dE_\gamma \propto E_\gamma^{-2.2}$, for $0.1 \text{ TeV} < E_\gamma < E_{\text{cut}} = 10 \text{ TeV}$ with isotropic energy $E_{\gamma,[0.1,10]}^{\text{iso}} = 3 \times 10^{53} \text{ erg}$ similarly to Ichiki et al. (2007). Such a large value may be rather optimistic (Albert et al. 2006), but possible if the strong synchrotron self-inverse Compton emission occurs. In this letter we shall adopt this value for demonstrations, and see, e.g.,

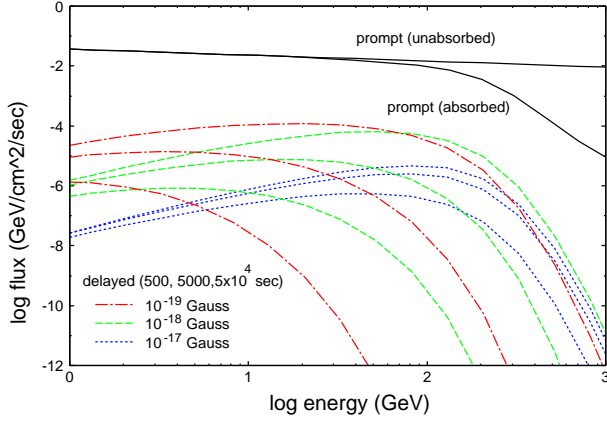


FIG. 1.— Typical spectra of pair echo emission at $t_{\text{obs}} = 500, 5000$ and 5×10^4 sec from a GRB located at $z = 0.3$. The coherence length of magnetic fields are set to $r_{\text{coh}} = 100$ pc. Other parameters are shown in the text.

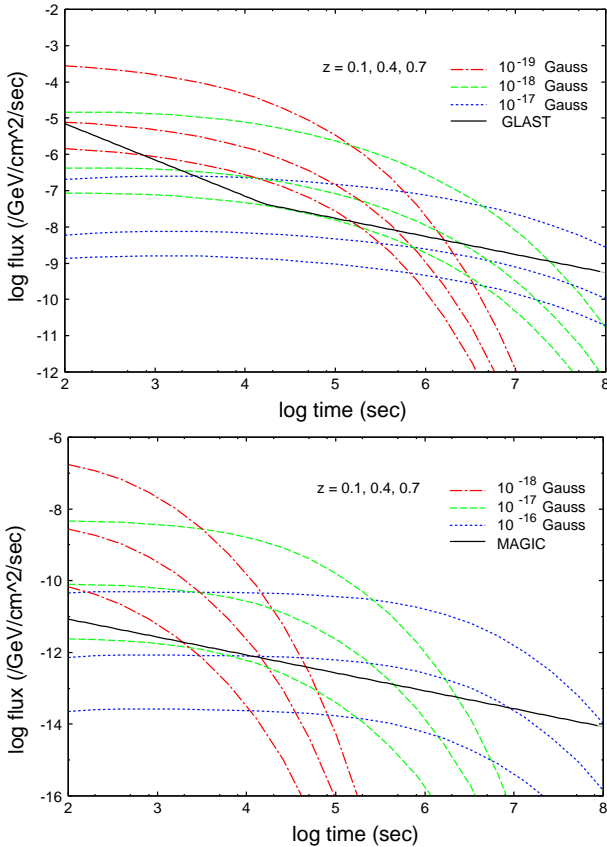


FIG. 2.— Typical light curves of pair echo emission at $E_{\text{delay}} = 1$ GeV (above) and $E_{\text{delay}} = 100$ GeV (below) from GRBs located at $z = 0.1, 0.4$ and 0.7 . The coherence length of magnetic fields are fixed to $r_{\text{coh}} = 100$ pc. Sensitivities of GLAST at 1 GeV (above) and MAGIC at 100 GeV (below) are also shown.

Murase et al. (2007) for more conservative cases. As to the density of ambient infrared photons, we adopted the "best fit" model developed by Kneiske et al. (2002, 2004) as a fiducial model. The sensitivities of GLAST and MAGIC are also shown in Fig. 2, respectively. As can be seen, the flux of pair echos decays exponentially with time scale estimated in Eq. (2).

It is important to note that the total fluence of pair echo emission is determined by the amount of absorbed primary

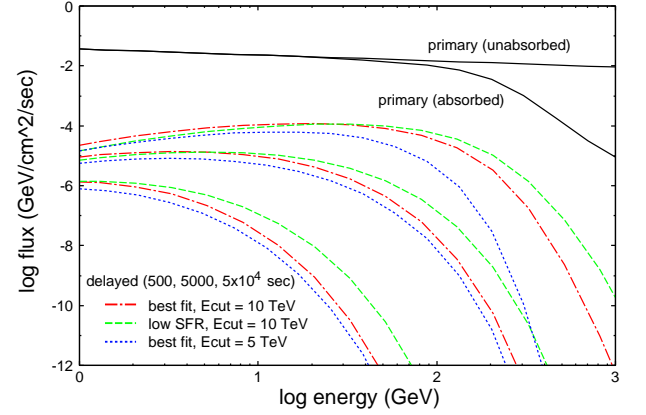


FIG. 3.— Comparison spectra of pair echo emission from a GRB located at $z = 0.3$ varying CIB model and E_{cut} . The magnitude and coherence length of magnetic fields are set to $B = 10^{-18}$ Gauss and $r_{\text{coh}} = 100$ pc, respectively. Other parameters are shown in the text.

gamma-rays and does not depend on the properties of magnetic field. On the other hand, the flux of pair echo emission is roughly the fluence divided by Δt and does depend on magnetic fields. From this fact, we see that there is an upper bound for the amplitude of magnetic field probed by our method. This is because strong magnetic fields lead to small flux of pair echo emission and make observations more difficult. The maximum measurable amplitude depends on several factors such as the distance of the source and detector sensitivity, and turns out to be typically about 10^{-16} G as we see later. Contrastingly, if magnetic fields are too weak, the time delay is dominated by angular spreading or hidden by the GRB duration, when we cannot obtain information on magnetic fields from pair echo emissions. The minimum measurable amplitude can be read from the ratios of delay times due to angular spreading and magnetic fields,

$$\frac{\Delta t_A}{\Delta t_B} = 1.5 \times 10^{-2} \left(\frac{E_{\text{echo}}}{1 \text{ GeV}} \right)^{1/2} \left(\frac{B}{10^{-18} \text{ G}} \right)^{-2} \left(\frac{r_{\text{coh}}}{100 \text{ pc}} \right)^{-1}. \quad (5)$$

Depending on the coherence length, the minimum measurable amplitude is expected to be $10^{-19} \sim 10^{-20}$ G. However, it should be noted that pair echo emission itself is easier to observe for weaker magnetic fields. Thus, we have both an upper bound and a lower bound for the measurable amplitude.

3. DETECTABILITY OF PAIR ECHO EMISSION FROM GRBS

As we stated in section 1, there are several factors which determine the flux of pair echo emission. First of all, as we saw in the previous section, strong magnetic fields and large coherence length lead to large time delay and hence low flux. Next, the density of CIB determines the amount of absorption of primary gamma-rays and then the flux of pair echos, but we have neither enough observational data nor theoretical understanding about it. Kneiske et al. (Kneiske et al. 2002, 2004) constructed several semi-empirical models of CIB evolution which well fit the observational data (see also Stecker et al. (2006)). In Fig. 3, we show the spectra of pair echos for their "low SFR" model, which predicts lower CIB density, compared to those for "best fit" model. There are two competing effects to understand the behavior of the spectra. Lower CIB density results in less absorption of primary gamma-rays and less pair echo emission, while re-absorption of pair echo emission, which is important at high energies, is also reduced.

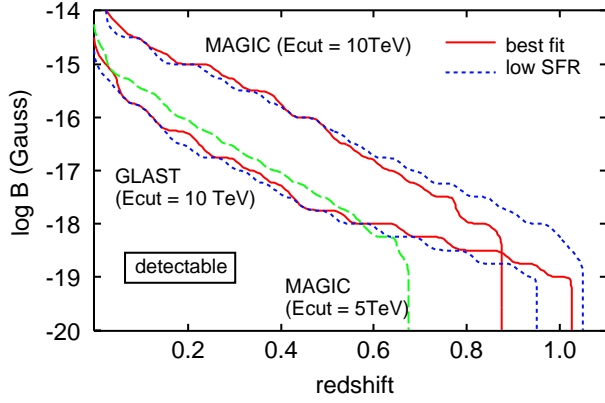


FIG. 4.— Detectable region of pair echo emission in z - B plane with GLAST and MAGIC for tangled magnetic fields with $r_{\text{coh}} = 100$ pc. Pair echo emission is considered to be detectable if the flux exceeds the detector sensitivity during the time between $10^2 \sim 10^7$ sec after the burst. Solid and dotted lines are estimations with "best fit" and "low SFR" models of CIB, respectively. Dashed line is for MAGIC with $E_{\text{cut}} = 5$ TeV and "best fit" CIB model.

In fact, contributions from upscattered CIB photons can also bring further complication (Murase et al. 2007).

Yet another uncertainty is E_{cut} . We show the spectra of pair echo emission for $E_{\text{cut}} = 5$ TeV also in Fig. 3. As one can understand from the typical relation between the energies of primary and pair echo gamma-rays, $\langle E_{\text{delay}} \rangle = 2.7 T_{\text{CMB}} \gamma_e^2 = 2.5 \text{ GeV} (E_{\gamma}/2 \text{ TeV})^2$, in the absence of high-energy primary gamma-rays, high-energy pair echo emission is substantially reduced at early phase. Contrastingly, dependence on E_{cut} is rather weak at late phase because late-phase pair echo emission is induced by low-energy primary gamma-rays.

In Fig. 4 we show regions in z - B plane where the flux of pair echo emission exceeds the detector sensitivities during the time interval $10^2 \text{ sec} \sim 10^7 \text{ sec}$, varying CIB model and E_{cut} . From Eqs. (2) we see that the delay time is shorter for higher energies so that MAGIC can probe stronger magnetic fields than GLAST. Below $B \sim 10^{-19}$ G, the detectability does not depend on B because the delay time is dominated by angular spreading or hidden by the GRB duration, and the flux above $\sim \text{GeV}$ energies does not depend on B . Dependence on E_{cut} is strong for MAGIC because its energy range is relatively high ($\gtrsim 100 \text{ GeV}$). In contrast, GLAST detects much lower-energy gamma-rays ($\lesssim 10 \text{ GeV}$) and is little affected by E_{cut} as long as it is high enough. Therefore, the detectability curve is not

shown for $E_{\text{cut}} = 5$ TeV, but of course it should be affected for even lower E_{cut} (Murase et al. 2007). Thus, we can see in the figure how large and small fields can be probed with GRBs with various redshift. For our specific GRB parameters which might be optimistic, the redshift must be rather small, $z \lesssim 1.0$, to detect pair echo emission. Since about 10% of GRBs will be located with $z \lesssim 1.0$, we expect that there would be some possibilities to probe magnetic fields with GRBs.

4. DISCUSSION AND SUMMARY

In this paper, we investigated the detectability of pair echo emission from gamma-ray bursts for GLAST and MAGIC. We calculated the spectra and light curves of pair echo emission using the formalism developed in (Ichiki et al. 2007) varying intergalactic magnetic fields, CIB model and cut-off energy. We showed the detectable region in (redshift)-(magnitude) plane and found that GLAST and MAGIC would be able to detect pair echo emission from GRBs with redshift $\lesssim 1$, while the cutoff energy will affect the detectability substantially for MAGIC. Thus, relatively nearby GRBs would allow us to probe high-energy emission of GRBs and properties of intergalactic magnetic fields.

One important ingredient which we did not discuss in detail is potential masking of pair echo emission by high-energy component of afterglow. While afterglows decays like power-law with time, pair echo emission lasts for a characteristic time determined by magnetic fields and then decays exponentially. Therefore, pair echo emission would tend to dominate afterglow at late phase, if intergalactic magnetic fields are relatively strong. As was pointed out in section 2, high-energy component of pair echo emission at late phase has a contribution from upscattered CIB. Thus, if pair echo emission at early phase would be masked by afterglow, the CIB contribution would become important in the argument of the detectability. This subject will be discussed in our future work.

The works of KT, KM and KI are supported by a Grant-in-Aid for the JSPS fellowship. The work of SN is supported by Grants-in-Aid for Scientific Research of the Japanese Ministry of Education, Culture, Sports, Science, and Technology 19104006, 19740139, 19047004. The numerical calculations were carried out on Altix3700 BX2 at YITP in Kyoto University.

REFERENCES

- Abdo, A. A. et al. 2007, *ApJ*, 666, 361
 Albert, J. et al. 2006, *ApJ*, 641, L9
 Ando, S. 2004, *MNRAS*, 354, 414
 Asano, K., & Inoue, S. 2007, *ApJ*, 671, 645
 Atkins, R. et al. 2000, *ApJ*, 533, L119
 Bamba, K., & Sasaki, M. 2007, *J. Cosmo. Astro-Part. Phys.*, 2, 30
 Casanova, S., Dingus, B. L., & Zhang, B. 2007, *ApJ*, 656, 306
 Dai, Z. G., & Lu, T. 2002, *ApJ*, 580, 1013
 Dai, Z. G., Zhang, B., Gou, L. J., Mészáros, P., & Waxman, E. 2002, *ApJ*, 580, L7
 Dermer, C. D., & Atoyan, A. 2004, *A&A*, 418, L5
 Fan, Y.-Z., Piran, T., Narayan, R., & Wei, D.-M. 2008, *MNRAS*, 384, 1483
 Gnedin, N. Y., Ferrara, A., & Zweibel, E. G. 2000, *ApJ*, 539, 505
 Guetta, D., & Granot, J. 2003, *ApJ*, 585, 885
 Hurley, K. et al. 1994, *Nature*, 372, 652
 Ichiki, K., Inoue, S., & Takahashi, K. 2007, *ApJ*, in press, arXiv:0711.1589
 Ichiki, K., Takahashi, K., Ohno, H., Hanayama, H., & Sugiyama, N. 2006, *Science*, 311, 827
 Kneiske, T. M., Bretz, T., Mannheim, K., & Hartmann, D. H. 2004, *A&A*, 413, 807
 Kneiske, T. M., Mannheim, K., & Hartmann, D. H. 2002, *A&A*, 386, 1
 Langer, M., Aghanim, N., & Puget, J.-L. 2005, *A&A*, 443, 367
 Maeda, S., Kitagawa, S., Kobayashi, T., & Shiromizu, T. 2008, *ArXiv e-prints*, arXiv:0805.0169
 Matarrese, S., Mollerach, S., Notari, A., & Riotto, A. 2005, *Phys. Rev. D*, 71, 043502
 Murase, K., Asano, K., & Nagataki, S. 2007, *ApJ*, 671, 1886
 Murase, K., & Ioka, K. 2008, *ApJ*, 676, 1123
 Murase, K., Ioka, K., Nagataki, S., & Nakamura, T. 2008, *Phys. Rev. D*, in press, 0801.2861
 Padilla, L. et al. 1998, *A&A*, 337, 43
 Papathanassiou, K., & Meszaros, P. 1996, *ApJ*, 471, L91
 Pe'er, A., & Waxman, E. 2004, *ApJ*, 613, 448
 Plaga, R. 1995, *Nature*, 374, 430
 Razzaque, S., Mészáros, P., & Zhang, B. 2004, *ApJ*, 613, 1072
 Sommer, M. et al. 1994, *ApJ*, 422, L63
 Stecker, F. W., Malkan, M. A., & Scully, S. T. 2006, *ApJ*, 648, 774

- Takahashi, K., Ichiki, K., Ohno, H., & Hanayama, H. 2005, Phys. Rev. Lett., 95, 121301
- Takahashi, K., Ichiki, K., & Sugiyama, N. 2007, ArXiv e-prints, arXiv:0710.4620
- The Tibet As Gamma Collaboration et al. 1996, A&A, 311, 919
- Totani, T. 1998, ApJ, 509, L81
- Turner, M. S., & Widrow, L. M. 1988, Phys. Rev. D, 37, 2743
- Wang, X. Y., Cheng, K. S., Dai, Z. G., & Lu, T. 2004, ApJ, 604, 306
- Wang, X. Y., Dai, Z. G., & Lu, T. 2001, ApJ, 546, L33
- Widrow, L. M. 2002, Rev. Mod. Phys. , 74, 775
- Zhang, B., & Mészáros, P. 2001, ApJ, 559, 110